4. DISCUSSIONS AND CONCLUSION

In this study, we presented and applied a focusing method based on hyperbolic summation (HS) technique to the simulated and measured B-scan GPR data generated via a SFR system, especially tested at C-band frequencies. The methodology was explained in detail and both numerical and measured examples, testing the effectiveness of the method, were presented. Application of the proposed method to the examples demonstrated that pipes and point scatterer-like objects produce very well-focused images in the new GPR image. This is due to the fact that the method uses hyperbolic templates corresponding to point-scatterers and converts these hyperbolas to single image pixels. The plate-like objects in the numerical examples also successfully produced well-focused images. In terms of computational efficiency, the algorithm is fast for 2-D B-scan images. It is clear that, the method can easily be adapted to 3-D C-scan images with hyperbolic surface templates. The method is examined with an SFR experimental set-up and measured B-scan GPR data. Both the traditional and the focused B-scan images were generated after applying the proposed method. Acceptable success has been achieved for the measured data as well.

The main weakness of the method becomes apparent for the case if any scattering mechanism falls under the hyperbolic template of another greater scattering, this point will produce a smaller scattering than its original EM energy in the final GPR image. Therefore, the energy levels in the final focused image will not correspond to the true energy levels of each scatterer. The other drawback of the method is that it produces ghost tails from the focused point toward upper regions as explained in Section 4. This phenomenon can be observed from Figure 5(b).

In this work, we only considered homogeneous and nearly lossless mediums. For inhomogeneous, lossy, and anisotropic mediums, the applicability of the method would be limited as the velocity and the wave number of the EM wave changes as the wave travels. Therefore, a model-based focusing method should be adopted for such soils.

REFERENCES

1. D.J. Daniels, Surface-penetrating radar, IEE Press, London, 1996.
2. L. Peters, Jr., D.J. Daniels, and J.D. Young, Ground penetrating radar as a subsurface environmental sensing tool, Proc IEEE 82 (1994), 1802–1822.
3. S. Vitebskiy, L. Carin, M.A. Ressler, and F.H. Le, Ultrawide-band, short pulse ground-penetrating radar: Simulation and measurement, IEEE Trans Geosci Remote Sens 35 (1997), 762–772.
4. L. Carin, N. Geng, M. McClure, J. Sichina, and L. Nguyen, Ultra-wide-band synthetic- aperture radar for mine-field detection, IEEE Trans Antennas Propag 41 (1999), 18–33.
5. J.I. Halman, K.A. Shubert, and G.T. Ruck, SAR processing of ground-penetrating radar data for buried UXO detection: Results from a surface-based system, IEEE Trans Antennas Propag 46 (1998), 1023–1027.
6. A. Sullivan, R. Damarla, N. Geng, Y. Dong, and L. Carin, Ultra wide-band synthetic aperture radar for detection of unexploded ordnance: Modeling and measurements, IEEE Trans Antennas Propag 48 (2000), 1306–1315.
7. C. Ozdemir, S. Lim, and H. Ling, A synthetic aperture algorithm for ground-penetrating radar imaging, Microwave Opt Tech Lett 42 (2004), 412–414.
8. E. Fisher, G.A. McMechan, A.P. Annan, and S.W. Cosway, Examples of reverse-time migration of single-channel, ground-penetrating radar profiles, Geophysics 57 (1992), 577–586.
9. L. Capineri, P. Grande, and J.A.G. Temple, Advanced image-processing technique for real-time interpretation of ground-penetrating radar images, Int J Imaging Syst Tech 9 (1998), 51–59.
10. C.J. Leuschen and R.G. Plumb, A matched-filter-based reverse-time migration algorithm for ground-penetrating radar data, IEEE Trans Geosci Remote Sens 39 (2001), 929–936.
11. I.L. Morrow and P.A. Van Genderen, 2D polarimetric backpropagation algorithm for ground-penetrating radar applications, Microwave Opt Technol Lett 28 (2001), 1–4.
12. O. Yilmaz, Seismic data processing, Society of Exploration Geophysicists, Tulsa, USA, 1987.
13. C. Cafforio, C. Prati, and F. Rocca, SAR data focusing using seismic migration techniques, Trans Aerospace Electron Syst 27 (1991), 194–206.
14. H. Ling, R. Chou, and S.W. Lee, Shooting and bouncing rays: Calculation the RCS of an arbitrary shaped cavity, IEEE Trans Antennas Propag 37 (1989), 194–205.
15. C. Ozdemir, R. Bhalla, L.C. Trintinalia, and H. Ling, ASAR—Antenna synthetic aperture radar imaging, IEEE Trans Antennas Propag 46 (1998), 1845–1852.
16. C. Ozdemir and H. Ling, ACSAR—Antenna coupling synthetic aperture radar imaging algorithm, J Electromagn Waves Appl 13 (1999), 285–306.

END-FED MODIFIED PLANAR DIPOLE ANTENNA FOR DTV SIGNAL RECEPTION

Yun-Wen Chi,[1] Kin-Lu Wong,[1] and Shih-Huang Yeh[2]
[1] Department of Electrical Engineering, National Sun Yat-Sen University, Kaohsiung 804, Taiwan
[2] Information and Communications Research Laboratories, Industrial Technology Research Institute, Hsinchu 310, Taiwan

ABSTRACT: *A novel end-fed modified planar dipole antenna for digital television (DTV) signal reception in the 470–806 MHz band is presented. The antenna is of a narrow rectangular shape (10 mm wide and 235 mm long) and is printed on a dielectric substrate. The antenna comprises a step-shaped radiating strip (arm 1) and a narrow rectangular radiating strip (arm 2), both separated by an L-shaped feed gap whose one open end located at the shorter edge or end edge of the antenna. Across this open end of the L-shaped feed gap, the antenna can be excited to provide a wide bandwidth (2.5:1 VSWR) of larger than 50%, which is much wider than that of a corresponding conventional center-fed dipole antenna and allows the proposed antenna easily cover the 470–806 MHz band for DTV signal reception. In addition, over the operating band, the radiation performance of the proposed antenna is similar to that of the conventional center-fed dipole antenna. The proposed end-fed modified planar dipole antenna is studied in detail in this paper.* © 2007 Wiley Periodicals, Inc. Microwave Opt Technol Lett 49: 676–680, 2007; Published online in Wiley InterScience (www.interscience.wiley.com). DOI 10.1002/mop.22229

Key words: *antennas; DTV antennas; dipole antennas; printed antennas; broadband antennas*

1. INTRODUCTION

In recent years, digital television (DTV) broadcasting has been operational in many countries [1]. Broadcasters are able to offer television with movie-quality picture and sound by using DTV system. In addition, DTV broadcasting can also provide multimedia and interactive services. With these advantageous features, it has become very attractive for wireless users to have their mobile communication devices such as the laptop computers, mobile phones, and personal media players to be equipped with a DTV receiver to enhance their multimedia functions [2–4]. Similarly, it is also very attractive for vehicle owners to have their vehicles equipped with a DTV device for receiving DTV programs [5, 6]. For these perspective trends, it is anticipated that a variety of mobile antennas for DTV signal reception will be increasingly required.

It is also noted that for horizontally polarized DTV signals [6], the horizontally oriented dipole antenna is a very promising candidate for DTV signal reception. However, conventional dipole antennas are usually with a narrow width, which makes it difficult to cover the DTV signal reception in the UHF band (470–806 MHz for channels 14–69 [7]). It is also noted that conventional dipole antennas are normally with a center-fed feeding structure. In this case, when the dipole antenna is attached horizontally onto the window pane of a vehicle for DTV signal reception, the feeding coaxial line for the center-fed dipole antenna cannot be easily concealed to achieve an aesthetical appearance.

In this paper, we present a novel end-fed modified planar dipole antenna having a wide bandwidth of larger than 50% for covering the 470–806 MHz band. For frequencies over the operating band, the proposed antenna shows similar radiation patterns as the conventional center-fed dipole antenna. Good radiation efficiency is also achieved for the proposed antenna. In addition, with the end-fed feeding structure, unlike the conventional center-fed feeding structure, the feeding coaxial line of the proposed antenna can be easily arranged to follow the edge of the window pane to achieve an aesthetical appearance, when the proposed antenna is horizontally attached on to the window pane of a vehicle. In this paper, details of the proposed antenna are described, and results of constructed prototypes are presented and discussed.

2. DESIGN CONSIDERATIONS OF PROPOSED ANTENNA

Figure 1 shows the proposed end-fed modified planar dipole antenna for DTV signal reception. The proposed antenna has a planar structure [8] and is printed on a 0.4-mm thick FR4 substrate with a narrow rectangular shape (width 10 mm and length L larger than 200 mm). Instead of using a central feed gap for a conventional dipole antenna, an L-shaped feed gap is used in the proposed antenna. The L-shaped feed gap also separates the proposed antenna into two arms (arm 1 and arm 2). One open end of the L-shaped feed gap is at the shorter edge or end edge of the antenna, while the other open end is at the longer edge of the antenna. Across the open end of the L-shaped feed gap at the end edge, the antenna is end-fed at points A and B by a 50 Ω coaxial line (not
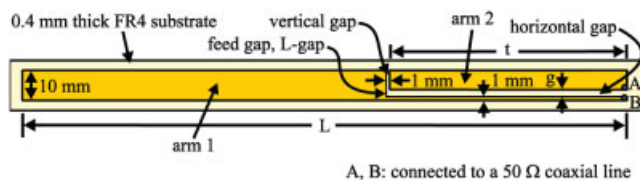
shown in the figure). Also note that, to eliminate the possible unbalanced surface currents flowing back from the antenna to the coaxial line to affect the measurement in the experiment, a balun element (not shown in the figure) is also connected in between the feeding points (points A and B) and the coaxial line.

Note that arms 1 and 2 are of different dimensions, different from the conventional dipole antenna with equal arms. In the proposed design, arms 1 and 2 are separated by the L-shaped feed gap, which comprises a vertical gap of width 1 mm and a horizontal gap of width g. Arm 1 is of a step shape and is formed by a wider portion of width 10 mm and a narrow portion of width 1 mm. In addition, the total length of arm 1 is L, the same as that of the antenna. For arm 2, it is of a simple rectangular shape and has a length of t and a width of 9 mm – g. By choosing proper values for the length L, the length t, and the gap width g for the proposed structure, a wide bandwidth (2.5:1 VSWR) of larger than 50% for the proposed antenna can be achieved. Both of the lengths L and t are found to have large effects on the lower and upper edge frequencies [f_L abd f_U, defined as the lowest and highest frequency with 2.5:1 VSWR over the band, respectively] of the obtained wide bandwidth. For the gap width g, it is found to mainly affect the upper edge frequency of the obtained wide bandwidth. Detailed effects of the parameters L, t, and g on the obtained bandwidth of the antenna will be explored with the aid of Figures 5–7 in the next section. Also note that for DTV signal reception, the bandwidth definition of 2.5:1 VSWR is generally acceptable for practical applications. In some cases, the definition of 3:1 VSWR has also been used [5].

Although the two arms of the proposed antenna are extended in the same direction, different from those of the conventional dipole antenna extended in the opposite directions, the radiation characteristics of the proposed antenna are found to be similar to those of the conventional dipole antenna. The proposed antenna is also found to operate in its fundamental resonant mode as a half-wavelength resonant structure determined by the total length ($L + t$) of the two arms. Hence, to achieve a lower edge frequency (f_L) to be about 470 MHz, the total length of $L + t$ is selected to be 309 mm (= 235 + 74 mm, which is about 0.48 wavelength of the frequency at 470 MHz) in the preferred design in this study.

Furthermore, it is found that the proposed antenna can generate an additional resonant mode at about 700–800 MHz, depending on the parameters of L, t, and g. This additional resonant mode and the fundamental resonant mode together are formed into a wide operating band, making it possible for the upper edge frequency (f_U) of the obtained bandwidth larger than 806 MHz. In this case, the obtained bandwidth of the proposed antenna can easily cover the 470–806 MHz band for DTV signal reception. More detailed characteristics of this additional resonant mode of the proposed antenna will be discussed with the aid of Figure 4 in the next section.

3. RESULTS AND DISCUSSION

The proposed antenna was constructed and tested. A preferred prototype with the length L, the length t, and the gap width g chosen to be 235, 74, and 3.5 mm was first constructed. Figure 2 shows the measured and simulated return loss for the constructed prototype. The simulated results are obtained using Ansoft simulation software HFSS (High Frequency Structure Simulator) [9], and agreement between the measured and simulated results is obtained. It is seen that the fundamental or the lowest resonant mode of the antenna is excited at about 510 MHz, and an additional resonant mode is occurred at about 740 MHz. These two resonant modes are formed into a wide operating band, with a bandwidth of 345 MHz (470–815 MHz) or about 54% centered at 640 MHz. This wide bandwidth covers the 470–806 MHz band for DTV signal reception.
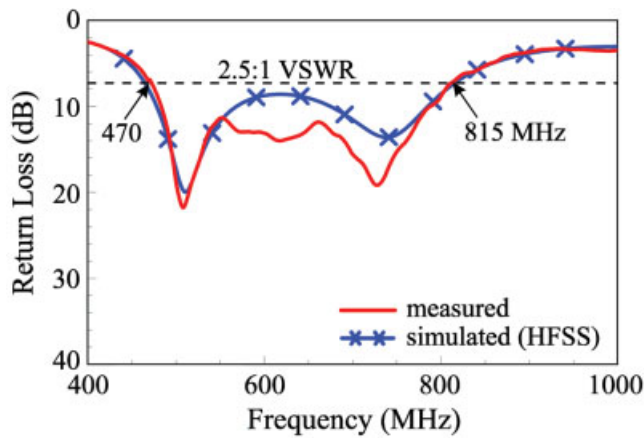

Figure 1 Configuration of the proposed end-fed modified planar dipole antenna for DTV signal reception. [Color figure can be viewed in the online issue, which is available at www.interscience.wiley.com]

Figure 2 Measured and simulated return loss for the proposed antenna; $L = 235$ mm, $t = 74$ mm, $g = 3.5$ mm. [Color figure can be viewed in the online issue, which is available at www.interscience.wiley.com]

Figure 4 Simulated excited surface currents at 510 and 740 MHz on the proposed antenna studied in Figure 2. [Color figure can be viewed in the online issue, which is available at www.interscience.wiley.com]

Figure 3 shows a comparison of the measured return loss for the proposed antenna studied in Figure 2 and the corresponding conventional center-fed dipole antenna (the reference antenna) shown in the inset in Figure 3. The length of the reference antenna is the same as that (235 mm) of the proposed antenna. For the reference antenna, a resonant mode at about 550 MHz is obtained. However, the obtained impedance bandwidth (120 MHz or about 22% centered at 550 MHz) is much smaller than that of the proposed antenna. The proposed antenna also shows a smaller lower edge frequency than that of the reference antenna.

Figure 4 shows the simulated excited surface currents at 510 and 740 MHz on the proposed antenna studied in Figure 2. The simulated results are also obtained using Ansoft simulation software HFSS. For the surface currents at 510 MHz, there are no null currents except at the end edges of arms 1 and 2. This suggests that the resonant mode excited at 510 MHz is the antenna's fundamental resonant mode. It is also found that the resonant frequency of this fundamental mode is mainly controlled by the total length ($L + t$) of arms 1 and 2 in the proposed antenna (see Figs. 5 and 6 in the following discussion). On the other hand, for the surface currents at 740 MHz, there is a null current at about the junction
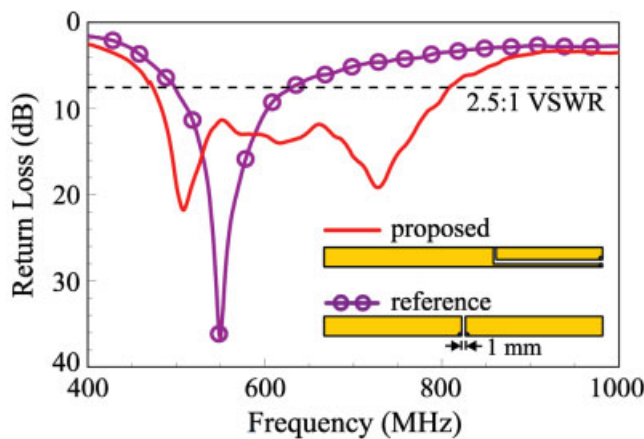
of the wide and narrow portions of arm 1. This indicates that the additional resonant mode excited at 740 MHz is the first higher-order mode of the proposed antenna. The successful excitation of the fundamental mode and the first higher-order mode in this study leads to a wide bandwidth obtained for the proposed antenna.

It should also be noted that the obtained wide bandwidth of the proposed antenna is strongly affected by the parameters L, t, and g. Effects of the length L are studied in Figure 5, in which the measured results of the return loss for L varied from 215 to 255 mm are shown. Other parameters are the same as studied in Figure 2. From the results, it is seen that a decrease in the length L will lead to an increase in the lower edge frequency f_L. This behavior is expected, since a smaller length L will make the resonant frequency of the antenna's fundamental mode shifted to higher frequencies. Similarly, it is seen that the upper edge frequency f_U is also shifted to higher frequencies. In addition, the increase in f_U is relatively much larger than f_L, thus resulting in a wider bandwidth obtained for a smaller length L. However, to make the obtained bandwidth covering the 470–806 MHz band, the length L was selected to be 235 MHz in this study.

Figure 3 Comparison of the measured return loss for the proposed antenna studied in Figure 2 and the corresponding conventional center-fed dipole antenna (the reference antenna, see inset in the figure). [Color figure can be viewed in the online issue, which is available at www.interscience.wiley.com]
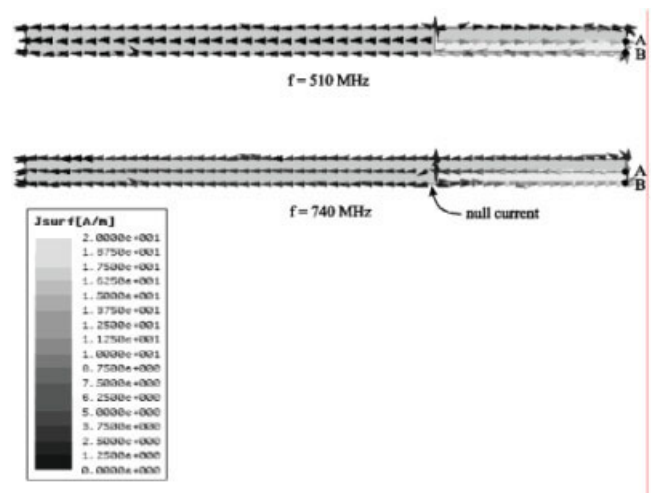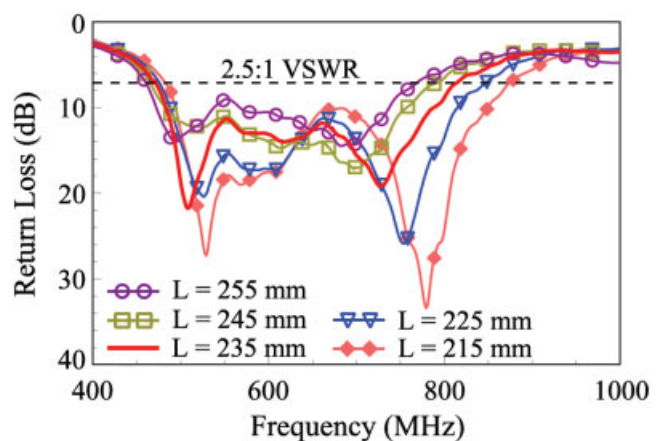

Figure 5 Measured return loss as a function of L, the length of arm 1. Other dimensions are the same as the antenna studied in Figure 2. [Color figure can be viewed in the online issue, which is available at www.interscience.wiley.com]
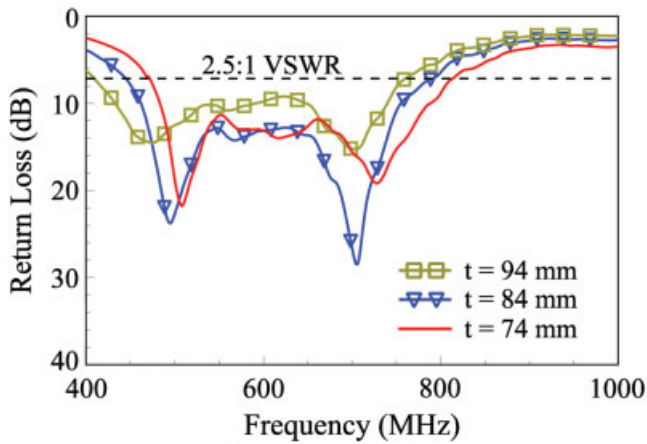
Figure 6 Measured return loss as a function of t, the length of arm 2. Other dimensions are the same as the antenna studied in Figure 2. [Color figure can be viewed in the online issue, which is available at www. interscience.wiley.com]

Figure 8 Simulated radiation patterns at 510 MHz for the antenna studied in Figure 2. [Color figure can be viewed in the online issue, which is available at www.interscience.wiley.com]

Figure 6 shows the effects of varying the length t of arm 2. The measured results of the return loss for t varied from 74 to 94 mm are presented. Similar to the effect of the length L studied in Figure 5, both of f_L and f_U are seen to increase with increasing length t. This indicates that, similar to the length L, the length t is also one of the major parameters controlling the impedance bandwidth of the proposed antenna. However, the increase in f_L and f_U is about the same, different from that observed in Figure 5.

Effects of the gap width g on the impedance matching of the proposed antenna are studied in Figure 7. Measured results of the return loss for g varied from 1.0 to 3.5 mm are presented. Other parameters are again the same as studied in Fig. 2. It is observed that the gap width g has small effects on the lower edge frequency of the obtained bandwidth. Conversely, large effects on the upper edge frequency are seen. This behavior is largely because the gap width g mainly affects the capacitive coupling between arms 1 and 2 and has small effects on the effective lengths of arms 1 and 2. The latter property leads to relatively very small effects on the upper edge frequency and the fundamental resonant mode of the proposed antenna. For the former property, it greatly affects the successful excitation of the additional resonant mode or the first
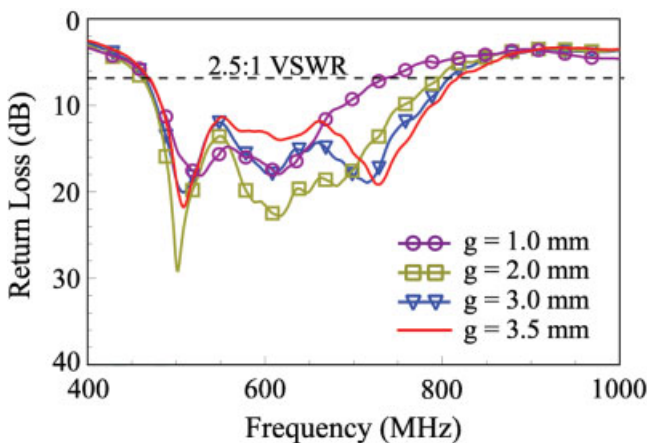
higher-order mode of the proposed antenna. The obtained results suggest that a larger gap width can lead to a good excitation of the first higher-order mode and thus result in a larger upper edge frequency. In this case, a wider bandwidth can be obtained.

Radiation characteristics of the proposed antenna were also studied. Since our anechoic chamber cannot operate at low frequencies such as in the DTV band of 470–806 MHz studied here, only the simulated results obtained using Ansoft simulation software HFSS are presented, which are expected to provide reliable results for the proposed antenna. Figures 8 and 9 plot the simulated radiation patterns at 510 and 740 MHz, respectively. The obtained radiation patterns are close to those of a conventional dipole antenna. Other frequencies over the 470–806 MHz band are also studied, and similar radiation patterns as plotted here are obtained. Figure 10 presents the simulated antenna gain and radiation efficiency over the operating band of the proposed antenna. Good antenna gain and radiation efficiency are obtained. The antenna

Figure 7 Measured return loss as a function of g, the width of the horizontal gap of the L-shaped feed gap. Other dimensions are the same as the antenna studied in Figure 2. [Color figure can be viewed in the online issue, which is available at www.interscience.wiley.com]
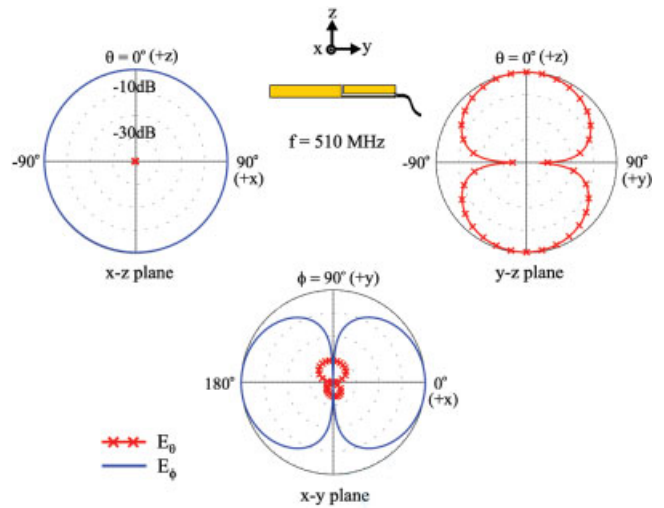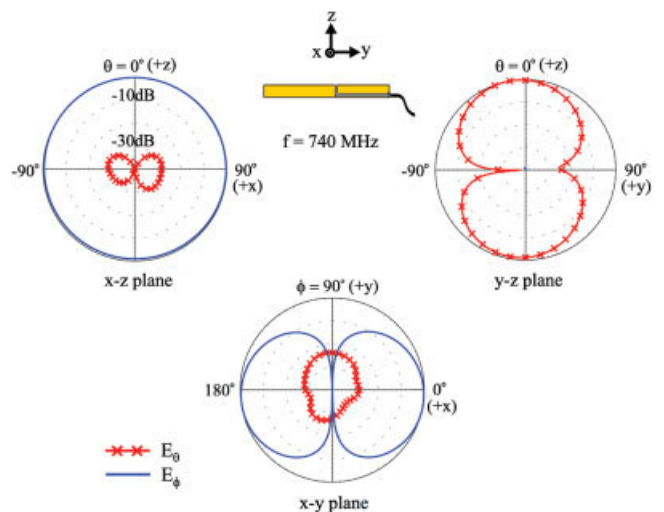

Figure 9 Simulated radiation patterns at 740 MHz for the antenna studied in Figure 2. [Color figure can be viewed in the online issue, which is available at www.interscience.wiley.com]
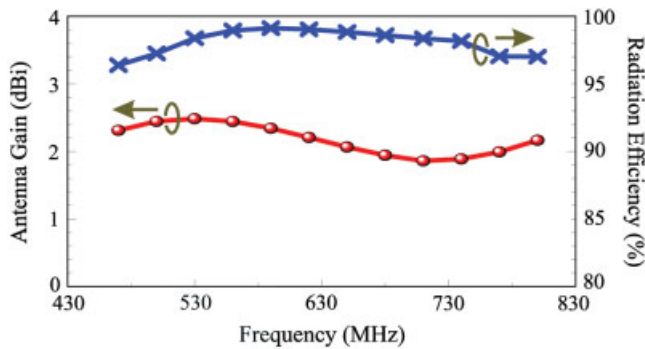
Figure 10 Simulated antenna gain and radiation efficiency for the antenna studied in Figure 2. [Color figure can be viewed in the online issue, which is available at www.interscience.wiley.com]

gain varies from about 1.8 to 2.5 dBi, and the radiation efficiency is all larger than 96% for frequencies over the band.

4. CONCLUSION

A novel end-fed modified planar dipole antenna for DTV signal reception in the 470–806 MHz band has been proposed and studied. Different from using a central feed gap for a conventional center-fed dipole antenna, the proposed antenna uses an L-shaped feed gap, which separates the antenna into two radiating arms of different lengths. With the proposed configuration, the antenna can be end-fed using a 50 Ω coaxial line. This property makes the proposed antenna very suitable to be attached onto the window pane of a vehicle for the reception of horizontally polarized DTV signals. In this case, the feeding coaxial line can be easily arranged to follow the edge of the window pane to achieve an aesthetical appearance. In addition, the proposed antenna can generate a wide bandwidth of larger than 50% to cover the 470–806 MHz band for DTV signal reception. This wide bandwidth is much larger than that (about 22%) of a corresponding center-fed dipole antenna. Moreover, over the obtained bandwidth, good dipole-like radiation characteristics have been obtained for the proposed antenna.

REFERENCES

1. http://www.fcc.gov/dtv/, Digital Television, Major Initiatives of Federal Communications Commission.
2. K.L. Wong, C.I. Lin, T.Y. Wu, J.W. Lai, and C.L. Tang, A planar DTV receiving antenna for laptop applications, Microwave Opt Technol Lett 42 (2004), 483–486.
3. C.M. Su, L.C. Chou, C.I. Lin, and K.L. Wong, Internal DTV receiving antenna for laptop application, Microwave Opt Technol Lett 44 (2005), 4–6.
4. K.L. Wong, Y.W. Chi, B. Chen, and S. Yang, Internal DTV antenna for folder-type mobile phone, Microwave Opt Technol Lett 48 (2006), 1015–1019.
5. T.J. Talty, Y. Dai, and L. Lanctot, Automotive antennas, trends and future requirement, In IEEE Antennas Propagat Soc Int Symp Dig, 2001, pp. 430–433.
6. H. Iizuka, T. Watanabe, K. Sato, and K. Nishikawa, Modified H-shaped antenna for automotive digital terrestrial reception, IEEE Trans Antennas Propagat 53 (2005), 2542–2548.
7. http://www.ntia.doc.gov/osmhome/allochrt.html, U.S. Frequency Allocations, Office of Spectrum Management, National Telecommunications and Information Administration, USA.
8. K. L. Wong, Planar antennas for wireless communications, Wiley, New York, 2003.
9. http://www.ansoft.com/products/hf/hfss/, Ansoft Corporation HFSS.

INTERNAL GSM/DCS DUAL-BAND OPEN-LOOP ANTENNA FOR LAPTOP APPLICATION

Cheng-Hao Kuo,[1] Kin-Lu Wong,[1] and Fa-Shian Chang[2]
[1] Department of Electrical Engineering, National Sun Yat-Sen University, Kaohsiung 804, Taiwan, Republic of China
[2] Department of Electrical Engineering, ROC Military Academy, Feng-Shan 830, Taiwan, Republic of China

ABSTRACT: *A novel open-loop antenna with a coupled-line gap for application as an internal laptop antenna for GSM/DCS dual-band operation is presented. Owing to the use of the coupled-line gap, the proposed antenna can operate both as a half-wavelength loop structure at 900 MHz and a one-wavelength loop structure at 1800 MHz. The antenna is easily printed on a dielectric substrate with a low cost and is then integrated to the supporting metal frame of the laptop display to achieve a compact size of 9 mm in height and 70 mm in length, making it very promising to be embedded within the casing of the laptop as an internal antenna. Design considerations of the proposed antenna are described, and experimental and simulation results of the constructed prototype are presented. Effects of the coupled-line gap on the dual-band operation of the proposed antenna are also analyzed.* © 2007 Wiley Periodicals, Inc. Microwave Opt Technol Lett 49: 680–684, 2007; Published online in Wiley InterScience (www.interscience.wiley.com). DOI 10.1002/mop.22224

1. INTRODUCTION

Many promising internal antennas for GSM (Global System for Mobile Communication, 890–960 MHz) and DCS (Digital Communication System, 1710–1880 MHz) operations have been studied and generally applied in the mobile phones [1]. Recently, it has been desired that the GSM/DCS internal antennas be applied in the laptop computers to achieve wireless internet access. In this case, with the added GSM/DCS internal antenna and the traditional 2.4/5 GHz internal antennas embedded in the laptop computers for WLAN (Wireless Local Area Network) operation [2–4], seamless or ubiquitous wireless network access [5] can be provided for wireless users with their laptop computers. However, the existing internal GSM/DCS mobile phone antennas are generally not applicable in the laptop computers. It is also noted that there are very few promising designs of the internal GSM/DCS laptop antennas available in the published papers.

Here in this paper, we report a novel dual-band open-loop antenna suitable for application as an internal laptop antenna for GSM/DCS operation. The proposed antenna has a simple configuration and is easy to fabricate by printing on a dielectric substrate. By integrating the proposed antenna to the supporting metal frame of the laptop display, a resonant loop path is formed for the proposed antenna. The resonant loop path is first designed to have a one-wavelength length of the desired higher frequency at 1800 MHz, which leads to a one-wavelength resonant mode excited for DCS operation. Then, by introducing a novel coupled-line gap at the proper location along the resonant loop path of the proposed antenna, a new half-wavelength resonant mode at about 900 MHz can be excited for GSM operation. Detailed configuration of the proposed dual-band open-loop antenna with a coupled-line gap is described in the paper. Effects of the coupled-line gap on the antenna's dual-band operation are also analyzed, and experimental results of the constructed prototype are presented and discussed.